BACKSCATTERING FROM A CUBE

A.C. LUDWIG
General Research Corporation
P.O. Box 6770, Santa Barbara, CA 93160

ABSTRACT

Three analytical techniques--the method of moments, geometrical theory of diffraction, and physical optics (without fringe current correction)--are applied to the case of backscattering from a cube. Results are compared to experimental data. It is relatively easy to compute specular scattering with good accuracy; it is much more difficult to obtain good accuracy for corner incidence, which is emphasized here precisely because it provides a more rigorous test of an analytical technique. As expected, the method of moments provides good results when the segmentation is on the order of 0.1 wavelengths, and in some cases up to 0.26 wavelengths. Single-diffraction geometrical theory of diffraction predicts peak scattering within a few dB for a cube dimension of 0.1-3 wavelengths, which is the full range of experimental data, but is not accurate between peaks. Physical optics predicts peak scattering within a few dB for a cube dimension of 1-3 wavelengths, and is also not accurate between peaks.

1 INTRODUCTION

A cube is a useful benchmark case for the class of scattering bodies consisting of flat faces. In this paper, monostatic backscattering is computed using the geometrical theory of diffraction (GTD) and physical optics (PO), which are nominally high frequency techniques, and the method of moments (MOM), which is nominally a low frequency technique. Experimental results are compared to the computed data.

This paper is not intended to be the final word on this subject; on the contrary, it has the modest goal of presenting a comparison of results obtained using a simple-minded application of currently available tools. GTD analysis was restricted to single-diffraction terms, physical optics was not corrected for fringe currents, and the NEC MOM code was used as is, without any real attempt to probe into reasons why results are good or bad. Bistatic scattering was not addressed. Any of these improvements would greatly increase the difficulty of the analysis. In summary, the goal of this paper is to address two questions: (1) how accurately can backscattering from a cube be calculated using a quick and dirty application of available techniques; and (2) what are the limitations of the techniques for a given size, incidence angle, etc.?

GTD and PO generally agree near specular reflections in directions normal to any of the faces of the body. Therefore, to discriminate between the techniques, the direction $\theta = 45°$, $\phi = 45°$ for the geometry of Fig. 1.1, which is about as far as possible from specular, is emphasized. For this angle, data were obtained for wavelengths λ such that the cube dimension a/λ ranges from 0.1 to 1.8 using MOM, and 0.1 to 10.0 for GTD and PO. However, as discussed below, no technique is accurate over the full computed range. Experimental data was obtained for the a/λ range of 0.1 to 3.0.

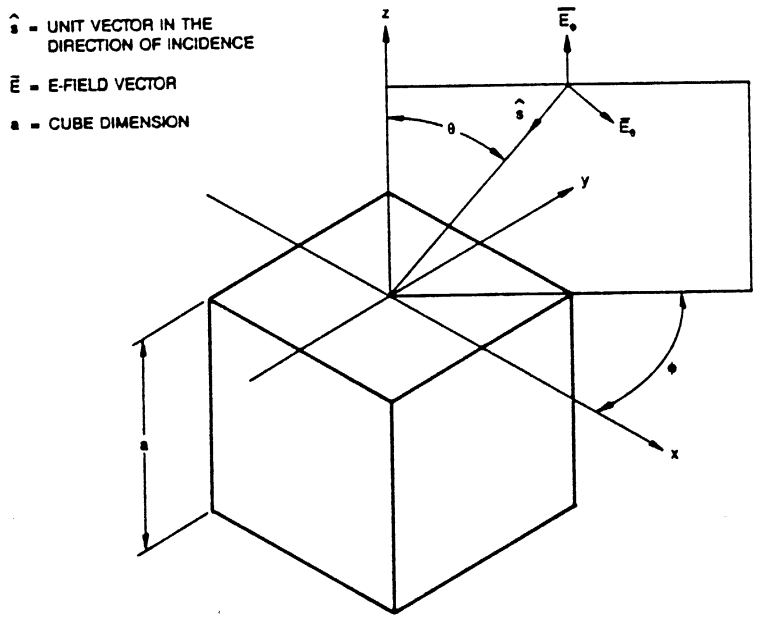

Figure 1.1. Global coordinate system.

2 METHOD OF MOMENTS COMPUTATION

The Livermore Numerical Electromagnetics Code [1] (NEC) was used for the method of moments calculations. This code includes both a patch model based on the magnetic field equation, and a wire grid model based on the electric field equation. For the patch model, each cube face was divided into 25 square patches of equal size, giving a total of 150 patches. For the wire model, the division was basically the same, but with the edges of each patch replaced by a wire, giving a total of 300 wires. The wire diameter was 0.0318a, to satisfy the "same surface area" criterion [2].

According to the NEC User's Manual [1], this patch subdivision should be good for a/λ up to 1.0, and the wire subdivision should be good for a/λ up to 0.5. As shown in Fig. 2.1, in fact the patch and

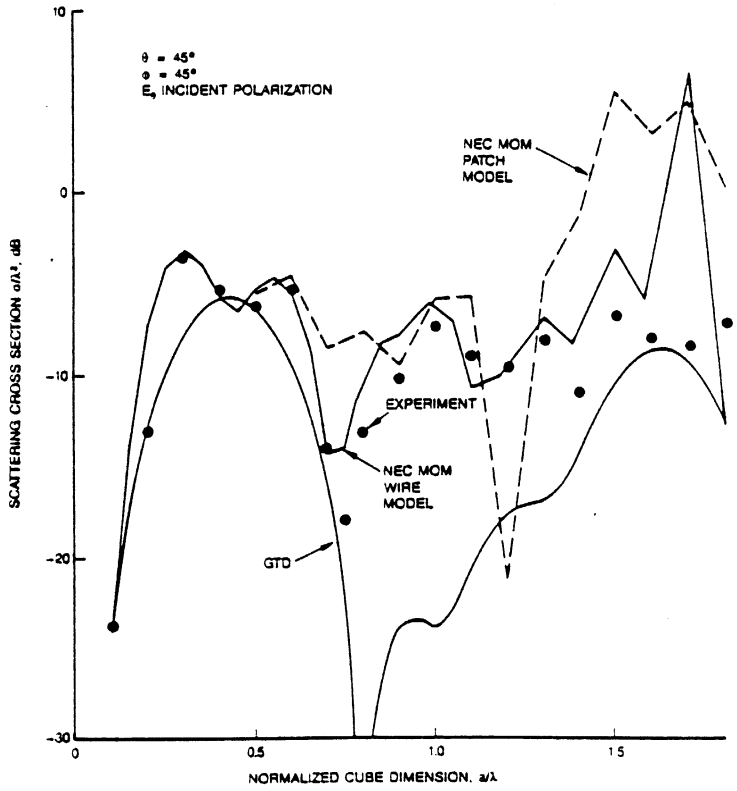

Figure 2.1. Cube monostatic backscattering versus a/λ .

wire grid results agree well up to $a/\lambda = 0.5$, but the experimental results agree better with the wire model results for $a/\lambda > 0.5$. (Also shown in the figure are GTD results which are discussed in the following section.) The experimental and analytical results shown in Fig. 2.1 have not been scaled in magnitude, and the agreement in absolute terms is excellent. For $a/\lambda > 1.0$, the MOM results diverge badly, which is not surprising. Of course, a finer patch subdivision could increase the range of accuracy, but the 300 by 300 matrix for the cases run here is close to the practical limits of the VAX 785 used to obtain the solution. Symmetry was not used to reduce the number of variables, and this would be a good way to extend the region of validity. Internal resonances are also a potential problem for $a/\lambda \geq 0.5$, and shorting these out would be another useful improvement.

In summary, the patch MOM results agree with the experimental results only up to $a/\lambda = 0.5$, which corresponds to a 0.1λ by 0.1λ patch size. Somewhat surprisingly, the wire model results agree reasonably well up to $a/\lambda = 1.3$, which corresponds to a wire grid segment length of 0.26λ . For larger values of a/λ , the wire grid and patch model MOM results diverge from each other and from the experimental results.

3 GEOMETRICAL THEORY OF DIFFRACTION COMPUTATION

The GTD computation was based on corner diffraction coefficients similar to those used by Sikta et al. [3]. The actual coefficients used were developed by Marhefka [4]. Only single diffraction terms were considered. It is well known that multiple diffraction is important for cube dimensions on the order of 1λ, so these results are certainly not representative of good GTD practice for small values of a/λ. However, the complexity of GTD analysis rises sharply when multiple diffraction is included, so these results do show what can be obtained with a relatively simple GTD analysis. For the case considered here, the diffracted field from each contribution is given by

$$E^d_{||} = -D_s E^i_{||} \frac{e^{-jks}}{s}$$

$$E^d_{\underline{|}} = -D_h E^i_{\underline{|}} \frac{e^{-jks}}{s} \qquad (3.1)$$

where superscripts d and i denote diffracted and incident fields, respectively; subscripts $||$ and $\underline{|}$ denote parallel and perpendicular field components, respectively

s is the two-way path length from the illumination source to the corner[1]

$k = 2\pi/\lambda$

D_s and D_h are the "soft" and "hard" diffraction coefficients

$\overline{E}_{||}$ and $\overline{E}_{\underline{|}}$ are parallel and perpendicular to the plane of incidence, defined with respect to a local coordinate system for each edge,

[1]The distance s is calculated using a "far-field" approximation so the source is implicitly assumed to be at an infinite distance from the cube.

as illustrated in Fig. 3.1. The unit vector $\hat{s}$ is in the direction of incidence; $\hat{s}$, $\overline{E}_{||}$ and $\overline{E}_{|}$ are mutually orthogonal. Also shown in Fig. 3.1 are the local incidence angles β_o and ϕ_o. The unit vector $\hat{s}$ is the same in both global and local coordinates (Figs. 1.1 and 3.1), but the field components and incidence angles in global and local coordinates are in general completely different. The explicit form for the diffraction coefficients are

$$D_n^s = \mp j \frac{\tan \beta_o}{8n\pi k} \left\{ \left| F\left[\frac{1}{2\pi \cos^2 \beta_o} \right] \right| 2 \cot \frac{\pi}{2n} \right. \tag{3.2}$$

$$\left. \mp \left| F\left[\frac{\cos^2 \phi_o}{2\pi \cos^2 \beta_o} \right] \right| \left(\cot \frac{\pi - 2\phi_o}{2n} + \cot \frac{\pi + 2\phi_o}{2n} \right) \right\}$$

where β_o and ϕ_o are as defined in Fig. 3.1

n is the wedge angle parameter; the internal wedge angle is $(2 - n)\pi$, so $n = 3/2$ for a cube, $n = 2$ for a flat plate

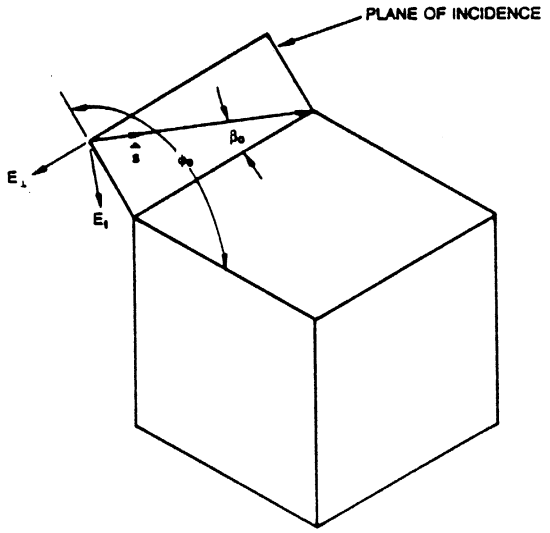

Figure 3.1. Local edge coordinate system.

and F is defined by

$$F[x] \equiv 2j|\sqrt{x}|e^{jx} \int_{|\sqrt{x}|}^{\infty} e^{-j\tau^2}\, d\tau \tag{3.3}$$

Each of the three edges forming a corner will make a contribution to the scattered field, if it is illuminated by the incident field. If the global incident angles are restricted to the quadrant

$$0 < \theta < \pi/2$$
$$0 < \phi < \pi/2 \tag{3.4}$$

then there will be 18 edge contributions, as illustrated in Fig. 3.2.

A computer program was written to evaluate the resultant of any subset of these contributions. For example, by selecting contributions

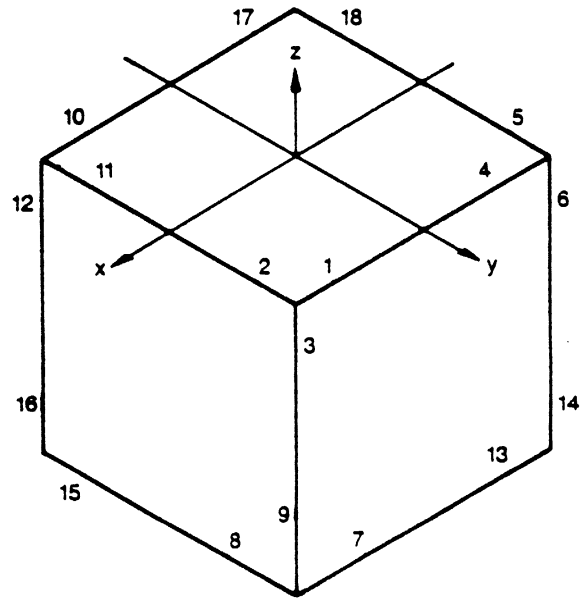

Figure 3.2. Eighteen edge contributions to the scattered field.

1, 3, 4, 6, 7, 9, 13, and 14, the scattering of just one face is obtained (see Fig. 3.2), and if the parameter n is set equal to 2, the result is the scattering of a square flat plate.[2] This was the case considered by Sikta et al. [3], and was used as the first test case; the new results agree well with Sikta et al., as shown in Fig. 3.3. For the

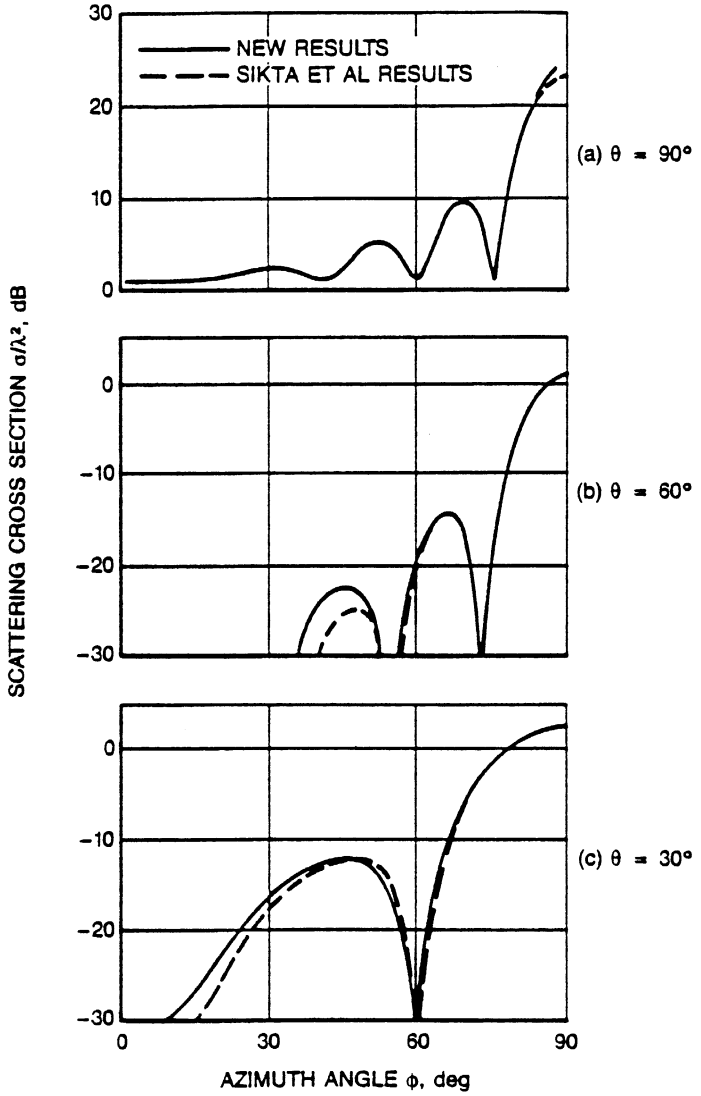

Figure 3.3. First test case: scattering from a 2λ by 2λ square flat plate.

[2] It is necessary to be careful that ϕ_o is calculated correctly when n values other than 1.5 are used.

second test case, the cube was modified to match a rectangular block evaluated by Ross et al., and reproduced by Kell and Ross [5]. The block dimensions are 14.763λ, 17.716λ , and 2.226λ in the x, y , and z directions, respectively. In this case, the new results are indistinguishable from Ross et al., as shown in Fig. 3.4.

The program was then applied to the $\theta = \phi = 45°$ case of particular interest here, with results as shown in Fig. 3.5. (Also shown in the figure are PO results which are discussed further in the following section.) It is seen that the computed scattering cross section varies over about a 30 dB range as frequency varies, but without a general systematic trend versus frequency. The results for $a/\lambda \leq 1.8$ are replicated in Fig. 2.1. The maximum level of the GTD scattering agrees with experiment within a few dB, but the details of the variation with frequency are not predicted well. Note that although the program agreed well with the first test case for a 2λ plate, Sikta et al. comment that "...many higher order terms are required for scattering outside the principal planes" [3].

The physical optics results also predict the maximum level within a few dB for a/λ between 1λ and 3λ ; the main divergence between PO and GTD is the deep nulls obtained with PO; however, neither GTD nor PO agree well with experiment in the null regions. The PO and GTD results for maximum scattering diverge by more than 10 dB for larger values of a/λ ; unfortunately, no experimental data are available in this range at this time. One potential difficulty in verifying the results experimentally up to $a/\lambda = 10$ is the sensitivity to alignment errors. Figure 3.6 shows a comparison of results where the azimuth and polar angles are varied by 1.0°. It is seen that the results vary by

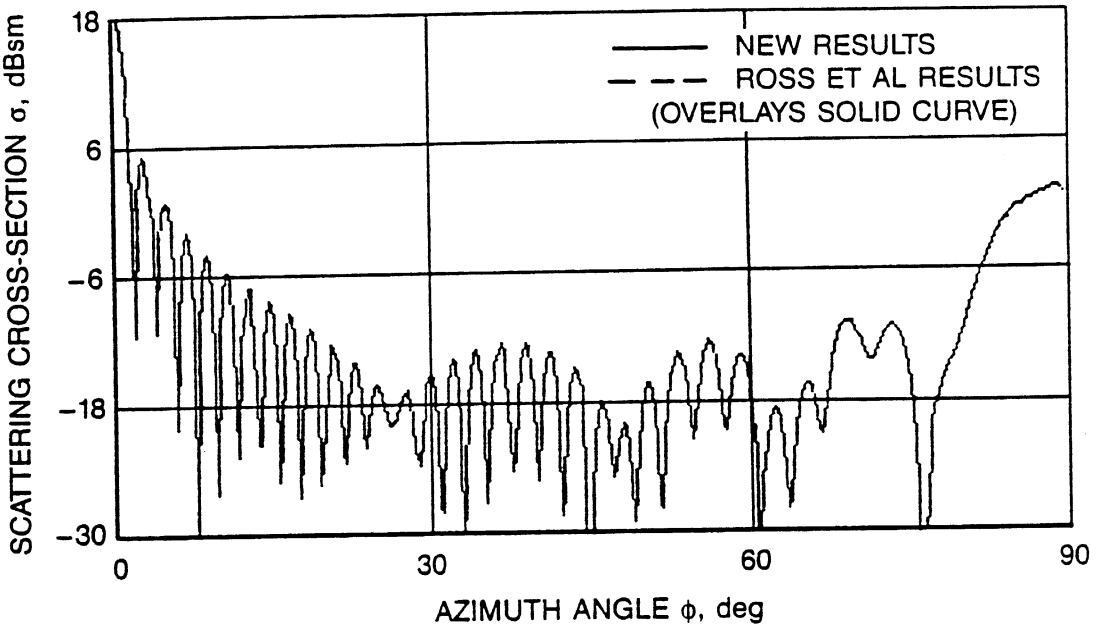

(a) E_ϕ polarization

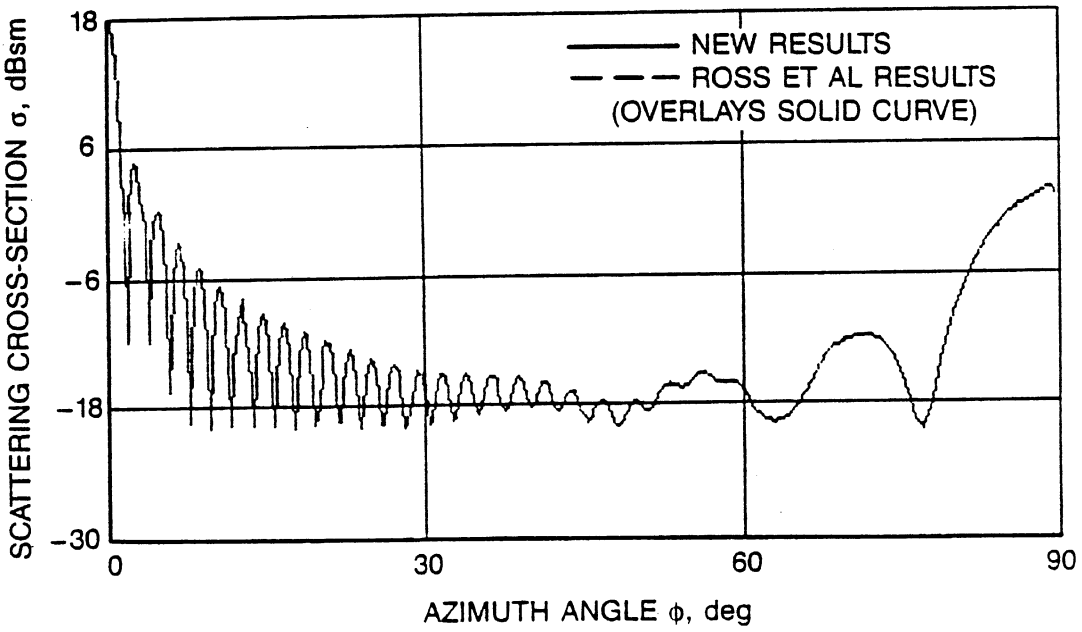

(b) E_θ polarization

Figure 3.4. Second test case: rectangular block.

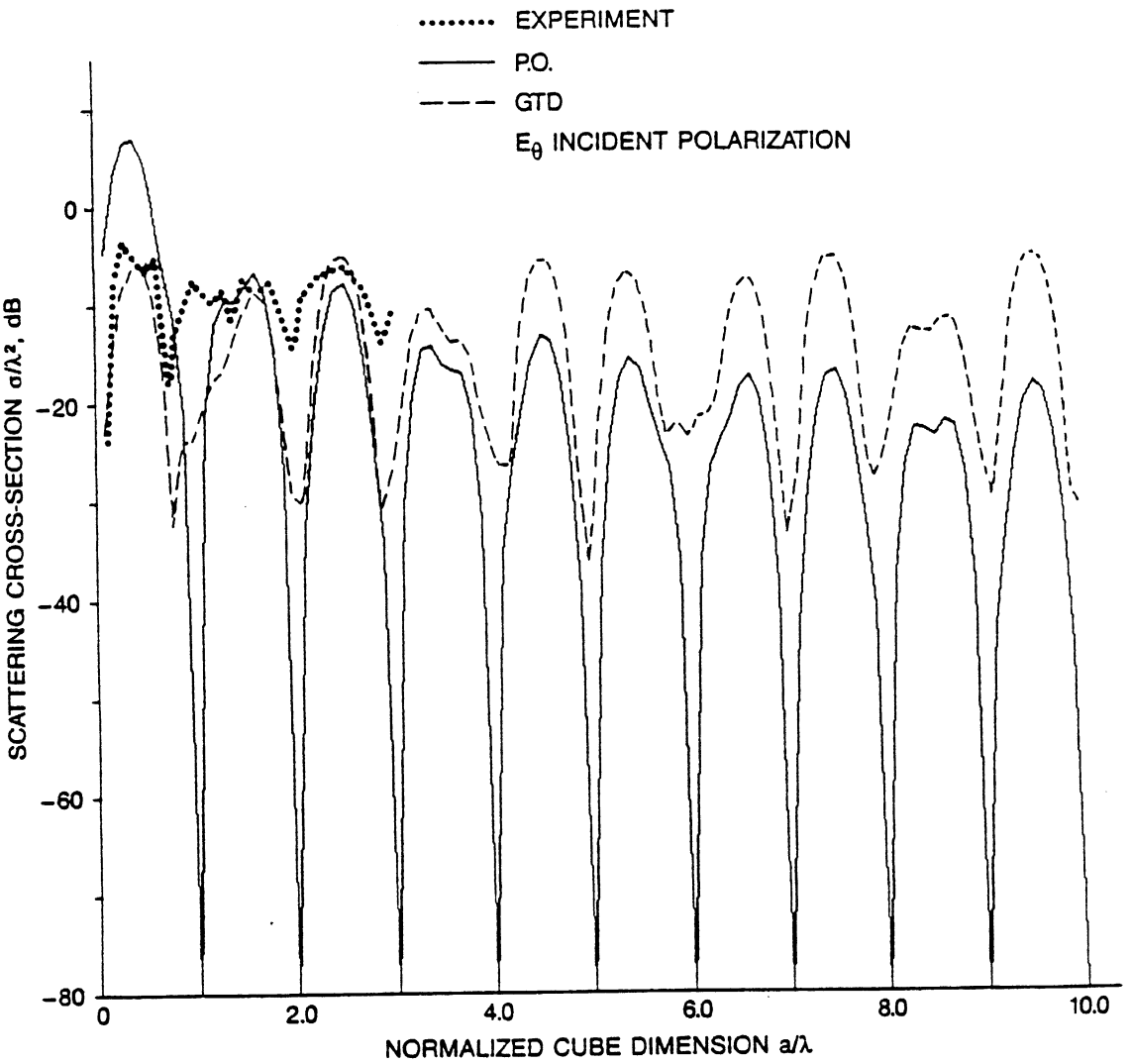

Figure 3.5. Cube scattering at $\theta = 45°$ and $\phi = 45°$ versus a/λ.

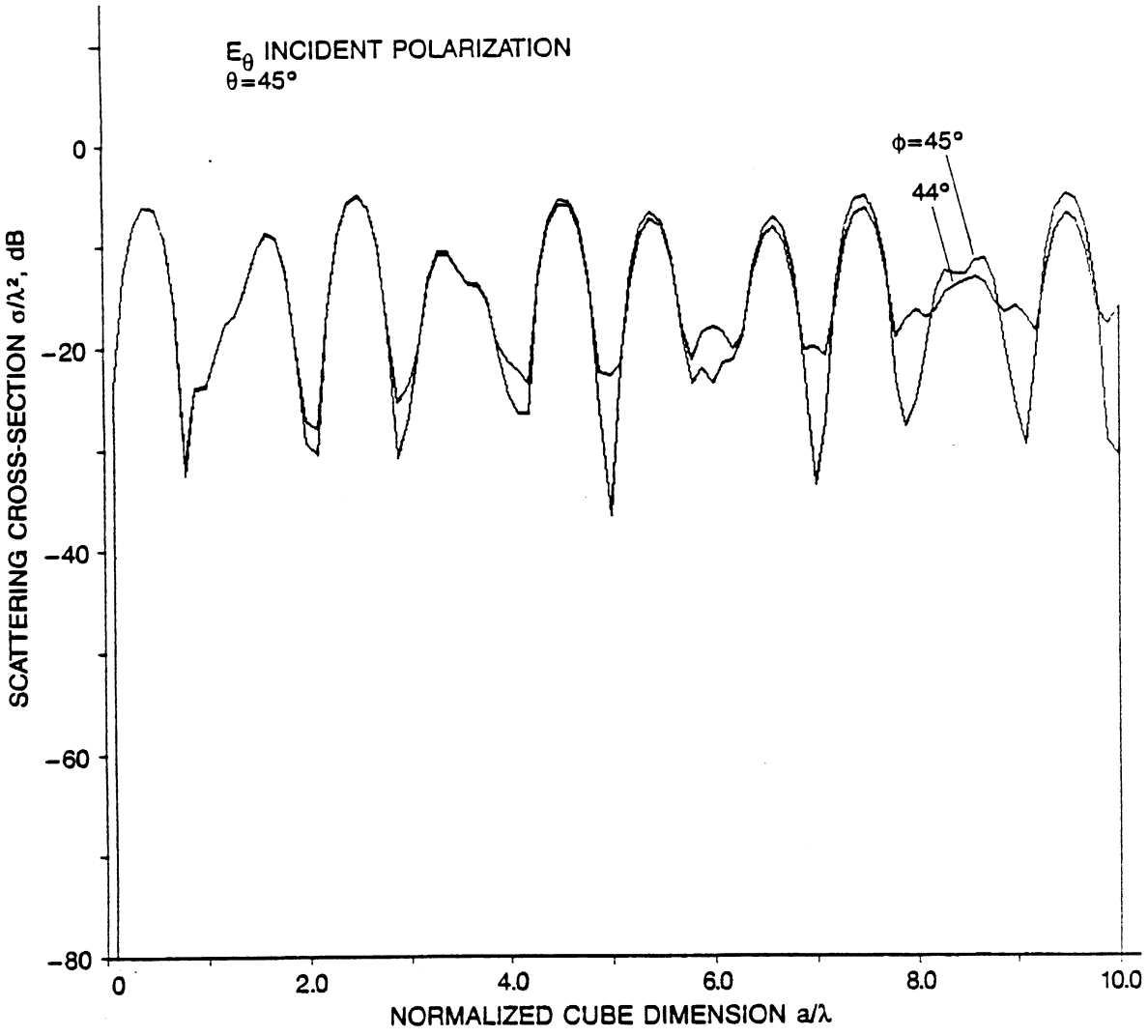

(a) Sensitivity to azimuth angle

Figure 3.6. Sensitivity of scattering results to angle errors.

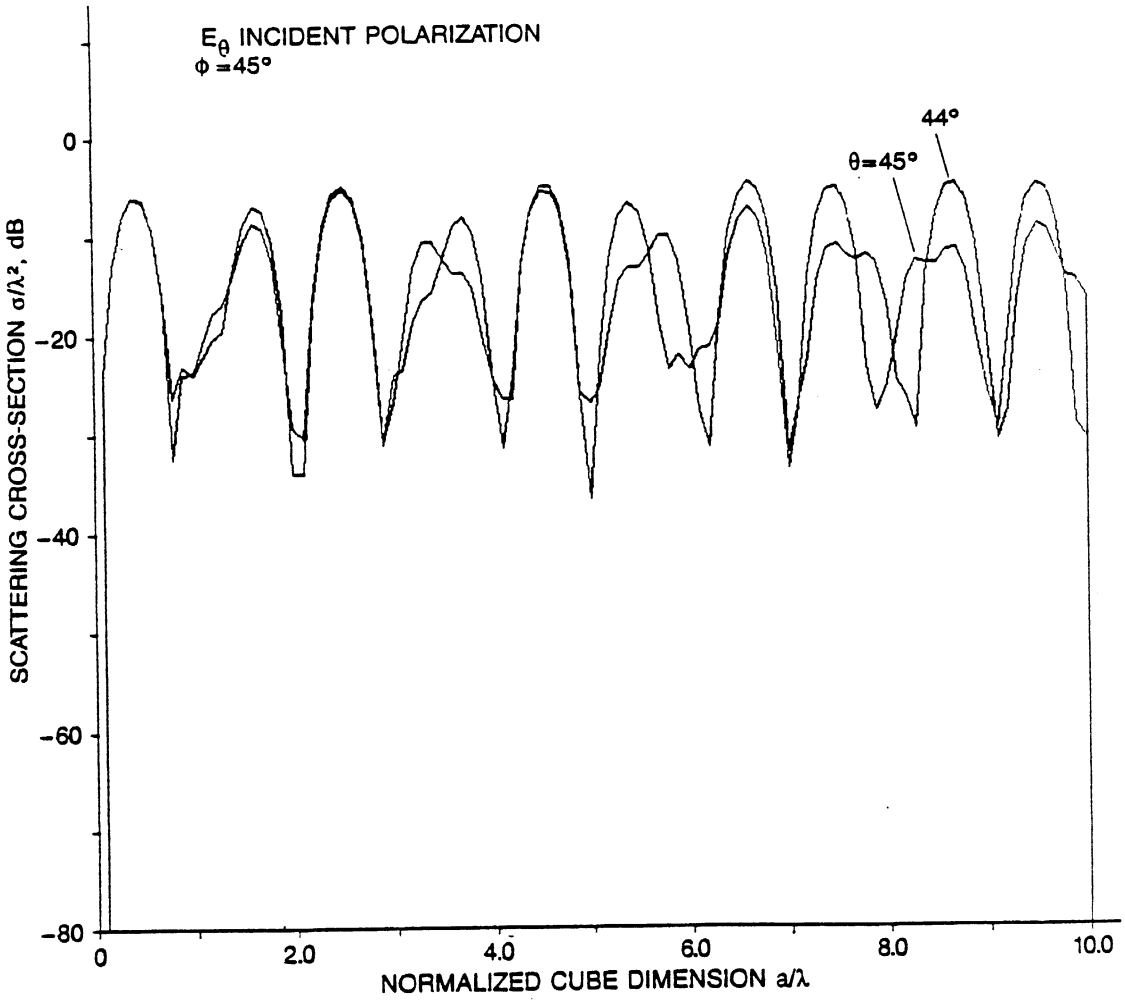

(b) Sensitivity to polar angle

Fig. 3.6 (Cont.)

several dB. Therefore, very careful angular alignment is required for a good verification.

As noted previously, the analytic and experimental results are not scaled and agree quite well in absolute terms. The analytic results are for monostatic backscattering; the experimental results were actually taken with a separate transmit and receive antenna with a 5-degree bistatic angle between them. This small bistatic angle probably accounts for some of the difference between experimental and calculated values at the larger values of a/λ . It would be useful to calculate the results for this bistatic angle to see how significant this is, or obtain true monostatic data, but this is left undone for this study.

4 PHYSICAL OPTICS COMPUTATION

The physical optics method is based on the approximation that on illuminated surfaces the currents $\overline{J}$ are given by

$$\overline{J} = 2\hat{n} \times \overline{H}_i \tag{4.1}$$

where $\overline{H}_i$ is the incident magnetic field. On shadowed surfaces, the currents are zero. The scattered field is then obtained by integrating the current contributions over the surface using standard equations [6]. It is well known that physical optics gives a poor approximation for the currents near edges and/or shadow boundaries; however, in spite of this, the bottom line results for the scattered fields are often a good approximation. It is generally accepted that GTD is more accurate than PO for this class of problems.[3] However, at the very least, PO provides an excellent check on GTD insofar as confirming the general character of the results, as shown below.

The scattering cross-section was calculated for a cube 10λ on a side for both a principal plane $\phi = 0°$, and for $\phi = 45°$; θ was varied over a $0° - 90°$ range. The PO results are compared with GTD results in Fig. 4.1. For this case, the physical optics results are identical for E_θ or E_ϕ incident polarization. The GTD results are not identical, but the comparison between PO and GTD is very similar for both polarizations; the E_θ polarization results are shown in Fig. 4.1. It is seen that the general features of the patterns agree quite well. However, in directions near nulls or near $\theta = 90°$ for the $\phi = 45°$ pattern, the results deviate by more than 20 dB.

The PO results at $\theta = 45°$ and $\phi = 45°$ versus a/λ have been shown previously in Fig. 3.5. Again, the general features agree well

[3] If PO is corrected for fringe currents using the Physical Theory of Diffraction (PTD), the accuracy may be comparable or superior to GTD—each technique has its advocates.

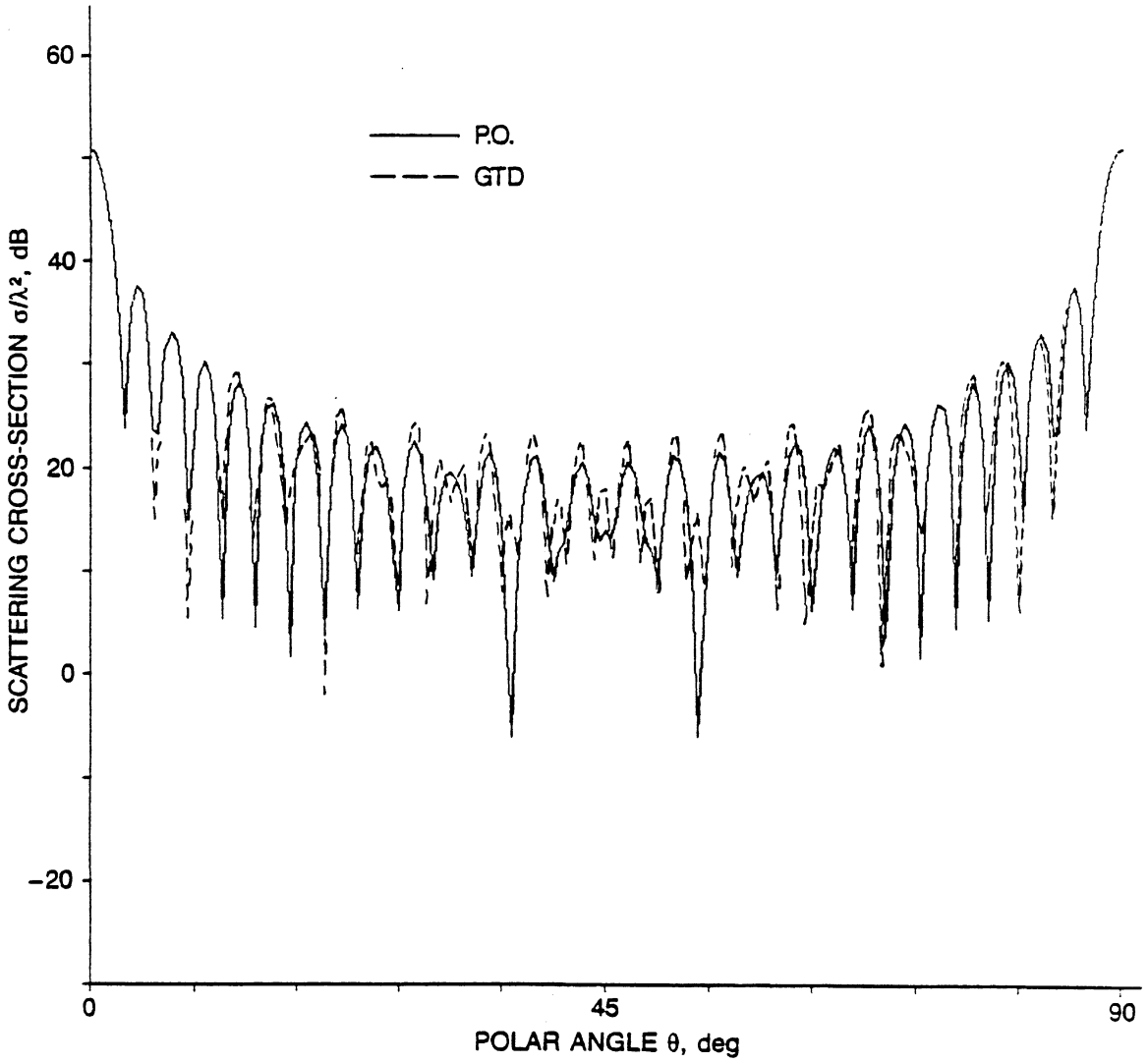

(a) $\phi = 0°$

Figure 4.1. PO and GTD results for a 10λ cube.

---

with GTD, but large deviations in level are evident. As mentioned above, it is generally believed that the GTD results are more accurate than PO.

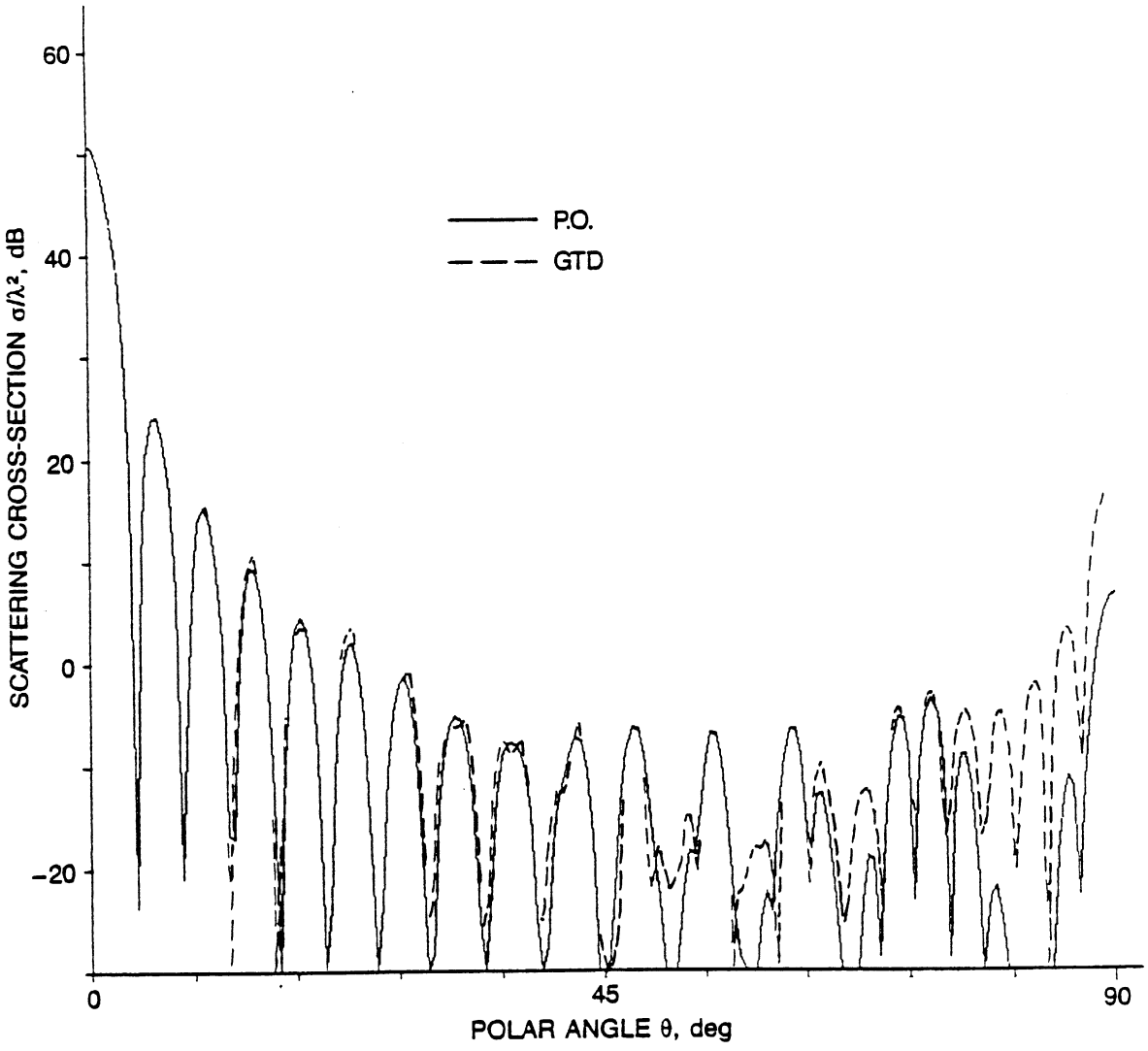

(b) $\phi = 45°$

Fig. 4.1 (Cont.)

5 SUMMARY AND CONCLUSIONS

The method of moments results are generally reliable only for segment lengths of 0.1λ or less, but the wire grid model provided good results up to a 0.26λ segment length. Single-diffraction GTD generally predicts the maximum values of backscattering versus frequency within a few dB over the entire range of experimental values--up to $a/\lambda = 3$--but does not accurately model behavior between maxima.

Physical optics results are surprisingly accurate for most scattering directions, and even for the $\theta = \phi = 45°$ direction are fairly accurate for $1 < a/\lambda < 3$; PO results diverge by roughly 10 dB from GTD results outside this range for the $\theta = \phi = 45°$ direction.

Experimental results for the larger values of a/λ would be valuable, but special care must be taken to assure good angular alignment.

A cube is as basic and elementary a shape as a sphere; scattering from a sphere can be calculated so accurately and reliably that calculated values are used as a standard to calibrate experiments; in contrast, no technique considered here is really satisfactory for calculating scattering from a cube. This appears to be a problem worthy of further attention.

ACKNOWLEDGEMENT

The author is indebted to Dr. Gail Flesher of General Research Corporation for the experimental results, which greatly enhance the value of the results presented in this paper.

REFERENCES

1. G.J. Burke and A.J. Pogio, "Numerical Electromagnetics Code (NEC)--Method of Moments," NOSC Technical Document 116, Naval Ocean Systems Center, San Diego, California, January 1981.

2. A.C. Ludwig, "Wire Grid Modeling of Surfaces," IEEE Trans. on Antennas and Propagation (to be published Sept 1987).

3. F.A. Sikta et al., "First-Order Equivalent Current and Corner Diffraction Scattering From Flat Plate Structures," IEEE Trans. on Antennas and Propagation, AP-37, No. 4, July 1983, pp. 584-589.

4. R. Marhefka, private communication, May 1986.

5. R.E. Kell and R.A. Ross, "Radar Cross Section of Targets," Chapter 27 of The Radar Handbook, M. Skolnik (Ed.), McGraw-Hill, 1970.

6. W.V.T. Rusch and P.P. Potter, Analysis of Reflector Antennas, Academic Press, New York, 1970.